Article

# Rechargeable Iron-Ion Battery Using a Pure Ionic Liquid Electrolyte

Yansong Zhao,* Yingpeng Zhen, and Tobias Boström

Cite This: *ACS Omega* 2022, 7, 24082−24090
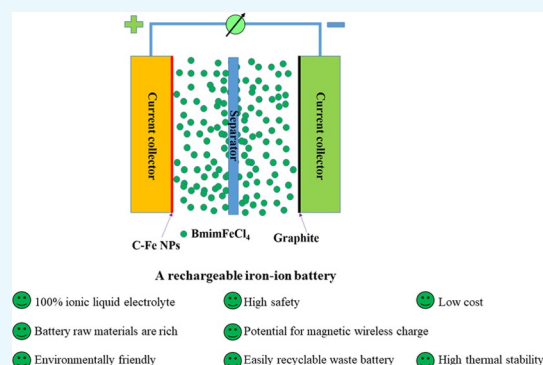
Read Online

ACCESS | Metrics & More | Article Recommendations

**ABSTRACT:** A rechargeable iron-ion battery (Fe-ion battery) has been fabricated in our laboratory using a pure ionic liquid electrolyte. Magnetic ionic liquids of 1-butyl-3-methylimidazolium tetrachloroferrate ($BmimFeCl_4$) and 1-methyl-3-octylimidazolium tetrachloroferrate ($OmimFeCl_4$) are synthesized and utilized as electrolytes in this work. The chemical structure of the two ionic liquids (ILs) is investigated using Raman analysis. In addition, the physical and thermal stability properties of the ionic liquid (IL) $BmimFeCl_4$, including density, viscosity, melting point, and decomposition temperature, are investigated using a density meter, viscosity meter, differential scanning calorimeter, and thermogravimetric analyzer. Moreover, the electrochemical properties, including electrochemical window, and ionic conductivity of the IL $BmimFeCl_4$ are investigated using an electrochemical instrument and a conductivity meter. It is found that the magnetic IL $BmimFeCl_4$ has good physical and electrochemical properties to be utilized as an electrolyte for iron-ion battery fabrication. Iron-containing materials, including pure iron foil, carbon-coated iron nanoparticles, and iron powder, are used as a cathode in the Fe-ion battery. The anode of the Fe-ion battery is graphite. Electrochemical properties of full cells are investigated, including cyclic voltammetry curves and specific charge−discharge capacity. The Fe-ion battery is a unique rechargeable ion battery with magnetic ions. In addition, pure IL $BmimFeCl_4$ is utilized as an electrolyte in this Fe-ion battery. IL $BmimFeCl_4$ is stable and almost nonvolatile. Therefore, an Fe-ion battery with a pure IL electrolyte is safer than that with an organic electrolyte. An Fe-ion battery using a pure IL electrolyte is a promising battery with many potential applications.

A rechargeable iron-ion battery

- 100% ionic liquid electrolyte
- Battery raw materials are rich
- Environmentally friendly
- High safety
- Potential for magnetic wireless charge
- Easily recyclable waste battery
- Low cost
- High thermal stability

## INTRODUCTION

Lithium (Li)-based batteries are becoming increasingly more important as energy storage devices in many applications. However, Li-based batteries have some disadvantages, for example, high cost, safety issues, and low abundance on the earth.[1,2] Therefore, many researchers have attempted to develop new types of batteries to solve the problems of Li-based batteries, including sodium batteries[3] and magnesium batteries.[4] However, the cost of sodium (Na) batteries and magnesium (Mg) batteries is still high. Actually, Fe is the cheapest metal among all of the metallic materials. In addition, there are plenty of mineable Fe on the earth, ca. 230 billion tons, which is about 15 000 times the amount of mineable Li on the earth. The element abundance of Fe ranks no.1 in the universe and no.2 on the earth among the metallic elements.[5,6] It means that there is plenty of Fe in the nature for the fabrication of iron-ion (Fe-ion) batteries. Therefore, Fe is the cheapest metal for the fabrication of new-generation batteries. The cost of Fe-ion batteries is potentially much lower than that of the other batteries mentioned above. In addition, Fe-ion batteries are extremely safe. The electrodes inside Fe-ion batteries are not oxygen- or water-sensitive. Fe-ion batteries are highly stable, and there is no explosion risk in Fe-ion batteries. In this work, we have developed a rechargeable Fe-ion battery.

Moreover, for the Fe-ion battery obtained in our laboratory, a pure ionic liquid (IL) is utilized as the electrolyte to replace the organic solvent electrolyte in the traditional batteries.

ILs are types of salts. Presently, ILs are a hot research topic. Several ILs are liquid at room temperature. Many ILs are liquid at temperatures as low as −60 °C and can be utilized in cold climate areas. ILs are regarded as environmentally friendly materials.[7,8] ILs have been utilized as novel and promising materials in many research fields,[9−11] including materials science, separation science, catalysis science, medicine science, and energy and climate technology. The utilization of ILs in energy conversion and energy storage, including solar cells,[12] batteries,[13] and supercapacitors,[14] is a crucial topic. ILs are utilized as electrolytes in batteries by many researchers to improve the performance of the current batteries.

In this work, electrolyte and electrode materials are selected for the fabrication of new-generation batteries. Pure IL

BmimFeCl$_4$ is utilized as an electrolyte in rechargeable Fe-ion batteries to replace the traditional organic solvents. IL BmimFeCl$_4$ can be easily obtained using a one-step synthesis method.[15,16] In addition, IL BmimFeCl$_4$ is very stable and is not water- or oxygen-sensitive. Moreover, the IL BmimFeCl$_4$ electrolyte is not flammable, which can significantly increase the safety property of batteries. The chemical structure and physical and thermal properties of IL BmimFeCl$_4$ are investigated by Raman analysis, differential scanning calorimetry (DSC), and thermogravimetric analysis (TGA) and using a density meter and viscosity meter. Electrochemical properties are important to utilize ILs as electrolytes. Therefore, in this work, the ionic conductivity of BmimFeCl$_4$ is investigated using a conductivity meter. The electrochemical window of BmimFeCl$_4$ is investigated using an electrochemical instrument.

Fe-ion batteries have a lot of potential applications, including stationary energy storage devices, buildings, railways, wireless charging smart roads, electrical cars, electric ships, mobile devices, space technology, and large-scale renewable energy storage systems.

## ■ EXPERIMENTAL SECTION

**Materials.** ILs of 1-butyl-3-methylimidazolium chloride (CAS R.N. 79917-90-1, BmimCl) and 1-methyl-3-octylimidazolium chloride (CAS R.N. 64697-40-1, OmimCl) were obtained from Sigma-Aldrich. The mass fraction purities of the two ILs were ≥97% and 97%, respectively. FeCl$_3$·6H$_2$O and Fe$_2$O$_3$ nanoparticles (average size: < 50 nm) were also purchased from Sigma-Aldrich. In addition, carbon-coated iron (C-Fe) nanoparticles (NPs) were purchased from Sigma-Aldrich and utilized for cathode preparation.

Sodium carboxymethyl cellulose (CMC, Dow Wolff Cellulosics), the conductive carbon black (Super C45, Super C60, IMER Graphite and Carbon), and graphite were also utilized for electrode preparation. Glass fiber was utilized as a separator in cells.

**Preparation and Treatment of IL Electrolytes.** ILs of BmimFeCl$_4$ and OmimFeCl$_4$ were synthesized in the laboratory according to our previous work.[16] Subsequently, the obtained ILs were dried in a dry room using the following method. All of the ILs were dried using the vacuum pump in a dry room. Water content in the dry room was <25 ppm. The drying procedure of ILs was as follows. First, an IL was dried in a dry room using a membrane pump for at least 2 days. The vacuum pressure of the final dried ILs was ca. $10^{-3}$ mbar. Subsequently, the predried IL was dried further using an extremely high vacuum ($10^{-7}$–$10^{-8}$ mbar) pressure pump to dry for at least 3 days at a certain temperature to remove the water and solvent in the IL. The water content of the final BmimFeCl$_4$ and OmimFeCl$_4$ obtained was less than 25 ppm.

**Density Measurement.** The density of BmimFeCl$_4$ was measured using a density meter (Anton Paar DMA 4100, Anton Paar Co., Austria). The temperature of this study was between 293.15 and 358.15 K at 5 K intervals. The temperature error was ±0.01 °C. The measurement was performed in a dry room (water content of the dry room was <25 ppm). The absolute room pressure was approximately 101 kPa during the measurement.

**Viscosity Measurement.** The viscosity of BmimFeCl$_4$ was measured using a rheometer (MCR 102, Anton Paar Modular Compact Rheometer). The viscosity of BmimFeCl$_4$ was

measured at shear rates ranging from 1 to 100 s$^{-1}$ at various temperatures ranging from 10 to 50 °C.

**Differential Scanning Calorimetry (DSC) Curve Measurement.** The melting point of BmimFeCl$_4$ was measured by DSC (Netzsch, Germany). The measurement procedure was as follows. A sample was loaded into the pan. The sample was cooled down to −150 °C. Subsequently, the sample was maintained at −150 °C for 5 min. Afterward, the sample was heated to −120 °C at a cooling rate of 5 °C/min and maintained at −120 °C for 5 min. Subsequently, the sample was heated to 20 °C at 1 °C/min, and the heat flow was measured during the process.

**Thermogravimetric Analysis (TGA) Curve Measurement.** The thermal stability of IL-based electrolytes was measured by TGA (TA instruments). A sample was loaded into the pan. Subsequently, the sample was maintained at 35 °C for 10 min. The sample was heated to 600 °C at a heating rate of 5 °C/min from 35 °C. Heat flow was measured during the heating process. The weight of the pan and sample is needed for the experiments.

**Raman Analysis.** The chemical structure of magnetic ILs of BmimFeCl$_4$ and OmimFeCl$_4$ was characterized by Raman spectroscopy (Vertex 70V, Bruker, Germany). A capillary was utilized for the measurement. One side of the capillary was closed, and the other side of the capillary was open. First, the capillary was kept in an oven at 120 °C in a dry room for at least 24 h to remove any water present inside of the capillary. Subsequently, the IL sample was filled into the capillary in an argon-filled glovebox. The water content and oxygen content in the glovebox were below 0.1 ppm. After the IL sample was filled into the capillary, the open side of the capillary was closed to form an isolated system. In the end, the capillary with the IL sample was loaded into the Raman spectrophotometer from the glovebox. Thus, the IL sample filled in the capillary cannot be influenced by the atmosphere, such as water, O$_2$, and CO$_2$. The measurement was performed at room temperature. The sample was filled into a capillary for the measurement.

**Ionic Conductivity Measurement.** The ionic conductivity of the BmimFeCl$_4$ electrolyte was measured using a conductivity meter at temperatures ranging from −30 to 100 °C. The temperature profile at ionic conductivity measurement was as follows. The temperature was increased from −30 to 100 °C. Subsequently, the temperature was decreased from 100 to 20 °C.

**Electrochemical Window Measurement.** The electrochemical window of the magnetic IL BmimFeCl$_4$ was measured using a multichannel potentiostat (Bio-Logic Science Instruments SAS, France). Experiments were performed at potential vs Ag/Ag$^+$ ranging from −5.0 to 5.0 V with a scanning rate of 0.5 mV/s. The working electrode was a Pt wire with a cross-sectional area of 0.0078 cm$^2$. The counter electrode was Ni (cross-sectional area: 1.13 cm$^2$). The reference electrode was a silver wire.

**Preparation of Cathode Materials.** Three different cathodes, including a pure Fe cathode, carbon-coated iron nanoparticles cathode (C-Fe cathode), and carbon reduced Fe$_2$O$_3$ cathode (Fe powder cathode), were utilized for the fabrication of Fe-ion batteries. The preparation methods for the three cathodes were shown as follows.

(a) Pure Fe cathode: Pure Fe (purity of ≥99.99% trace metals basis) was purchased from Sigma-Aldrich. Pure Fe was utilized as a cathode for the Fe-ion battery.

(b) C-Fe cathode: The C-Fe cathode was prepared as follows. Step 1: CMC was dissolved in $H_2O$ to form a gel-like sample by stirring for at least 2 h. Step 2: The carbon-coated Fe NPs and carbon 45 were added to the gel-like sample. Afterward, the sample was stirred for at least 12 h to obtain a slurry. Step 3: The slurry was coated on the surface of a Ni foil using a doctor blade to form a 200 $\mu$m thin film. Step 4: The Ni foil with the thin film was heated at 80 °C for at least 12 h to remove the water. Step 5: The Ni foil with the thin film was cut to obtain C-Fe electrodes. Afterward, the C-Fe electrodes were further dried using a high vacuum pump. Finally, the C-Fe electrodes were obtained for battery preparation.

(c) Fe powder cathode: The preparation method of the Fe powder cathode is similar to that of the C-Fe cathode. However, in Step 2, the Fe powder reduced from $Fe_2O_3$ by carbon 45 was added to the gel-like sample. The reduced Fe powder was prepared as follows: the mixture of $Fe_2O_3$, sucrose, and super C65 was burnt at 1000 °C for 1 h to obtain a powder, and the powder was utilized for cathode preparation. The rest of the steps of Fe powder cathode preparation are similar to those of C-Fe cathode preparation.

**Anode Material Preparation.** Graphite was utilized as an anode in Fe-ion batteries. The graphite electrode preparation process was as follows. Step 1: CMC was dissolved in $H_2O$ to form a gel-like sample by stirring for at least 2 h. Step 2: Graphite and carbon 45 were added to the gel-like sample. Afterward, the sample was stirred for at least 12 h to obtain a slurry. Step 3: The slurry was coated as a 150 $\mu$m thin film on the surface of a Ni foil using a doctor blade. Step 4: The Ni foil with a thin graphite film was heated at 80 °C for at least 12 h to remove the water. Step 5: The Ni foil with the thin graphite film was cut into graphite electrodes. Afterward, the graphite electrode was further dried using a high vacuum pump. Finally, the graphite electrodes were obtained for battery preparation.

**Electrolyte Preparation.** Magnetic ILs of 1-butyl-3-methylimidazolium tetrachloroferrate ($BmimFeCl_4$) and 1-methyl-3-octylimidazolium tetrachloroferrate ($OmimFeCl_4$) were synthesized in the laboratory according to our previous work.[16] Subsequently, the water content of the ILs was removed in a dry room of our laboratory using a high vacuum pump.

**Current Collector Selection.** The current collectors for the electrode preparation were chosen between Cu, Ni, and Al foils. A Ni−Ni symmetric cell, a Cu-Cu symmetric cell, and an Al-Al symmetric cell were prepared. The electrolyte utilized in the cells was $BmimFeCl_4$. All of the symmetric cells were fabricated in an argon-filled glovebox (MBRAUN UNIlab; $H_2O$ content <0.1 ppm, $O_2$ content <0.1 ppm) filled with ultrapure argon. The cyclic voltammetry (CV) test of the three symmetric cells was performed using a galvanostat/potentiostat VMP (Bio-Logic, France). In addition, a graphite−graphite symmetric cell was prepared. The electrolyte in the cell was pure $BmimFeCl_4$. Subsequently, the CV test of the graphite−graphite cell was performed.
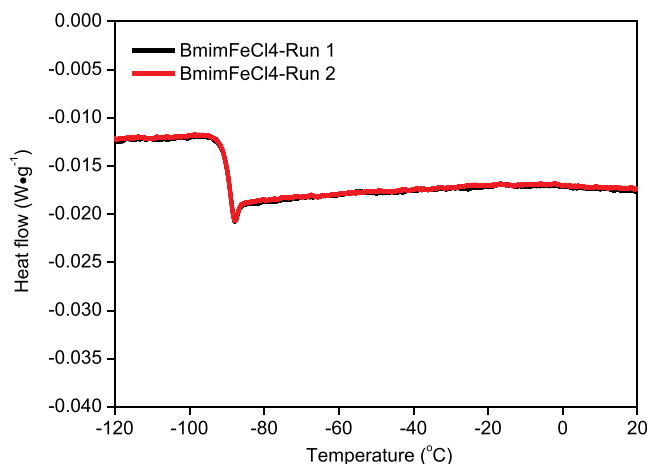
**Corrosion Test.** The corrosion effect of $BmimFeCl_4$ on Cu, Al, and Ni foils was investigated in a dry room (water content
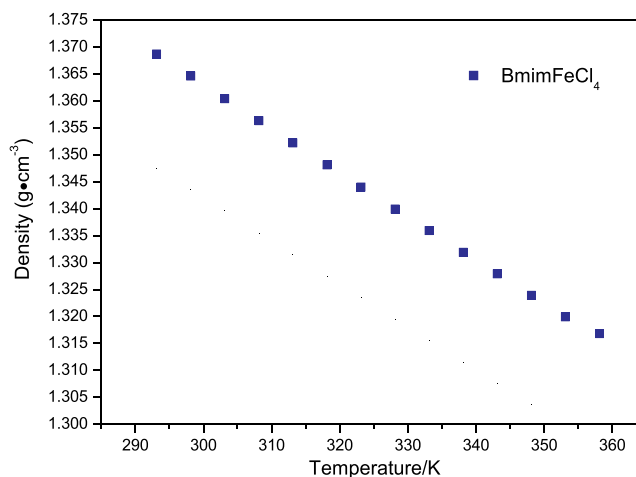


**Figure 1.** Density of $BmimFeCl_4$ at temperatures from 20 to 80 °C.
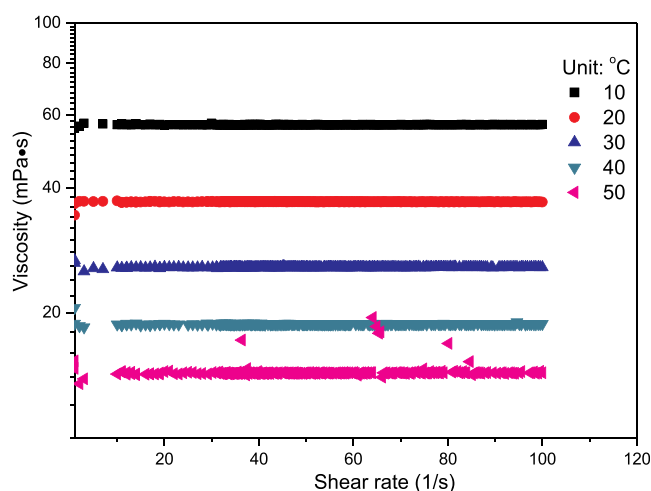


**Figure 2.** Viscosity of $BmimFeCl_4$ at temperatures ranging from 10 to 50 °C.



**Figure 3.** DSC curves for $BimFeCl_4$ and crystalline temperature determination.

<25 ppm) at our laboratory. In this test, first, Cu, Al, and Ni foils were put into three experimental vials, respectively. Subsequently, two drops of $BmimFeCl_4$ were placed on the surface of Cu, Al, and Ni foils. In addition, there were reference Cu, Al, and Ni foils without $BmimFeCl_4$ on the surface. The
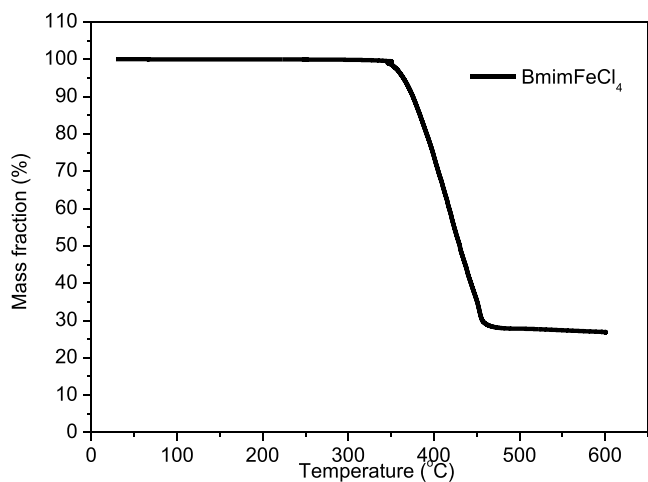
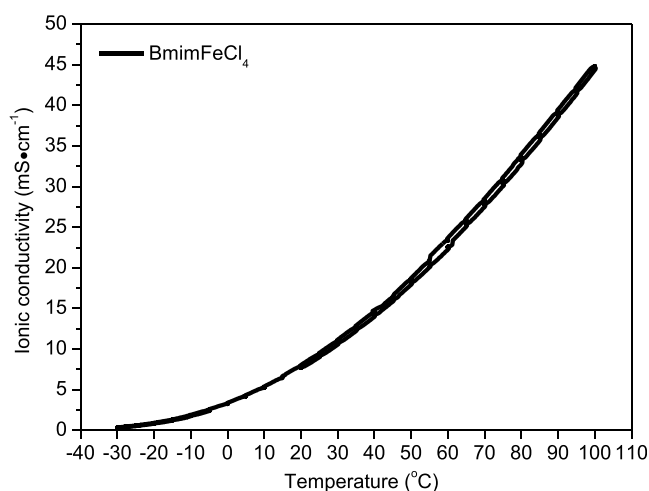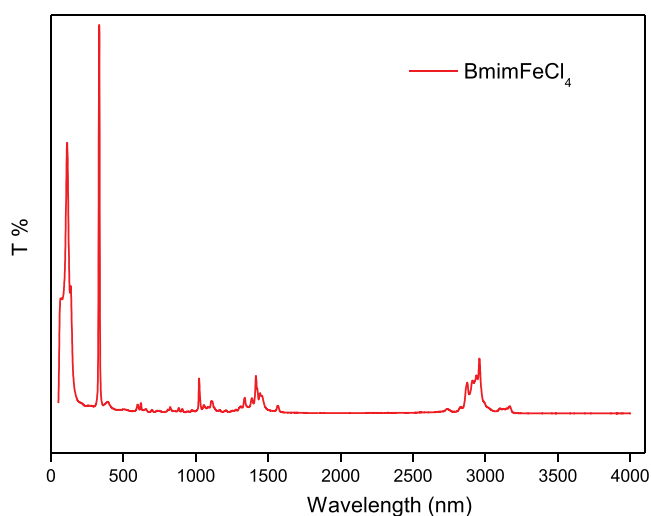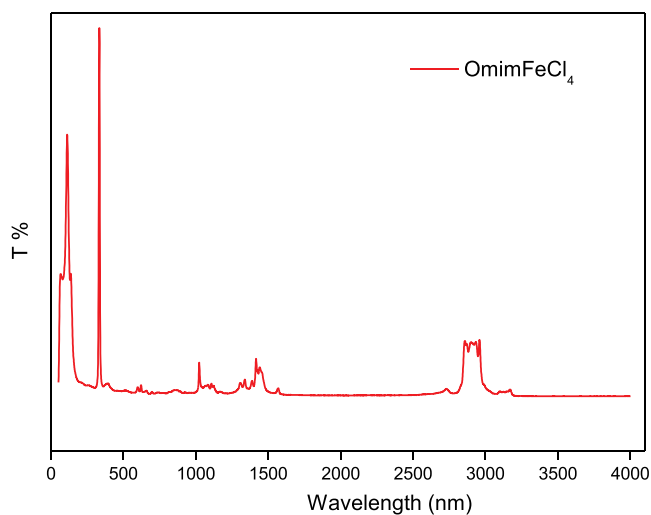**Figure 4.** TGA curves of IL BmimFeCl$_4$.



**Figure 6.** Ionic conductivity measurement of IL BmimFeCl$_4$.
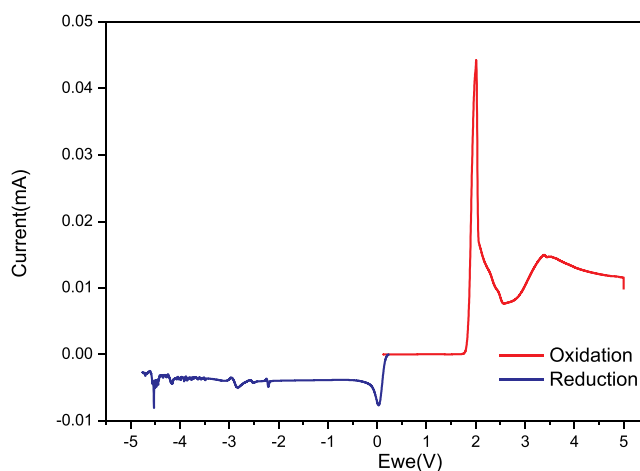


(a)



**Figure 7.** Electrochemical window measurement of IL BmimFeCl$_4$.

foils with and without BmimFeCl$_4$ were kept quiescently on a laboratory bench for 40 days at room temperature. In the end, the foil surface photos were taken during the corrosion test.

**CV Test of the Fe-Graphite Full Cell.** The Fe-Fe symmetric cell, C-Fe-C-Fe symmetric cell, and Fe powder-Fe powder symmetric cells were prepared for CV tests. The electrolyte in the symmetric cells was BmimFeCl$_4$. The test was performed using a VMP.

**Charge and Discharge of the Full Cell.** All of the galvanostatic charge–discharge experiments were performed using a Maccor Battery Tester 4300. Three full cells of the Fe graphite cell, C-Fe graphite cell, and Fe powder graphite were prepared for the charge and discharge test. The electrolyte in the symmetric cells was BmimFeCl$_4$. The reference electrode was Ag.

**SEM.** The morphology of the electrode materials utilized in this work was characterized using a SEM (SEM, ZEISS 1550VP field emission scanning electron microscope operated at 5 kV). The experiments were performed at room temperature.



(b)

**Figure 5.** Raman analysis of magnetic ILs: (a) BmimFeCl$_4$ and (b) OmimFeCl$_4$.

■ **RESULTS AND DISCUSSION**

**Density Measurement.** The density of BmimFeCl$_4$ was measured using a density meter in this work. The density data
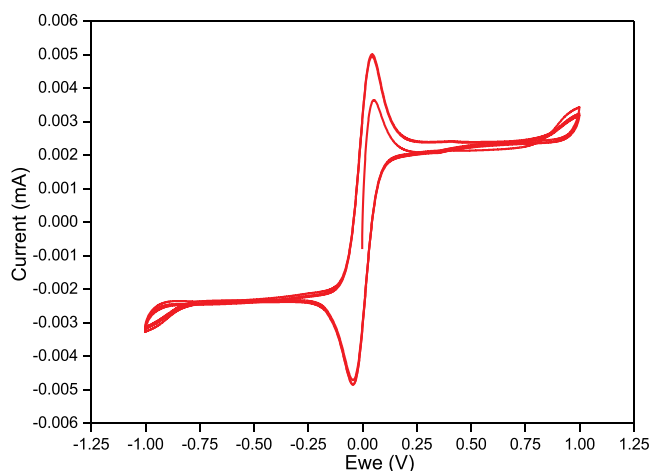
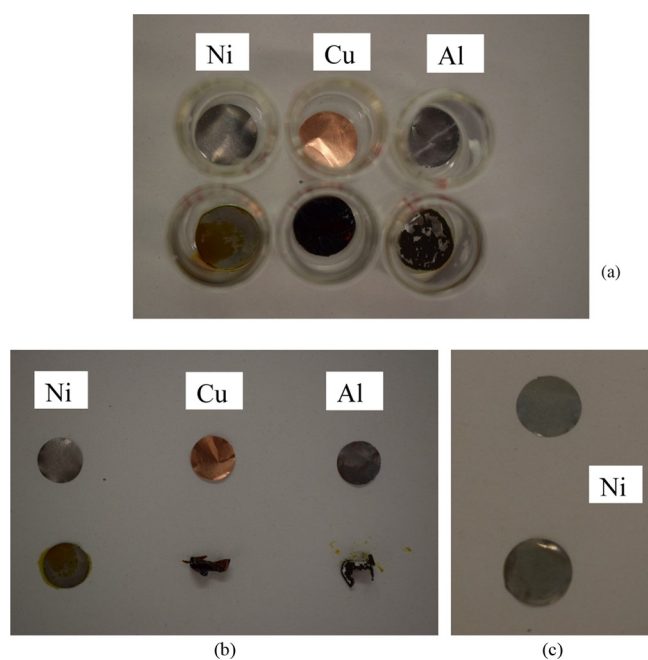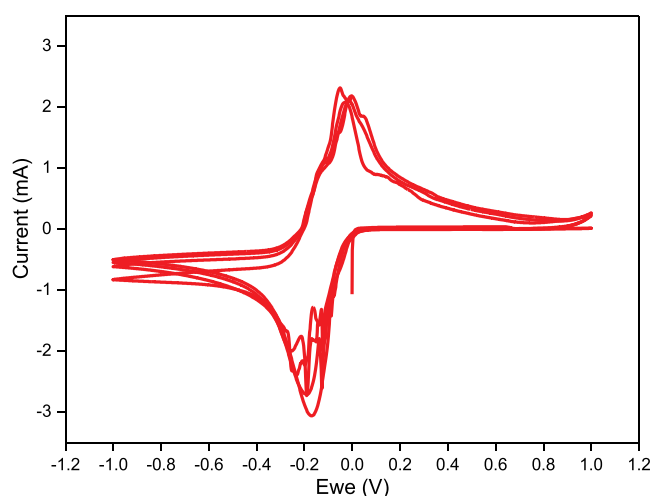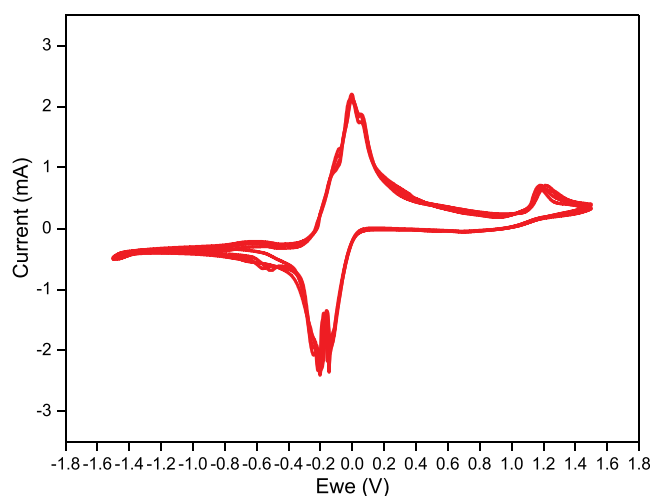**Figure 8.** CV test of the Ni-Ni symmetric cell.



**Figure 9.** Corrosion test of BmimFeCl$_4$ on Cu, Al, and Ni. (a) Fresh metal foil without BmimFeCl$_4$ (upper) and with BmimFeCl$_4$ (lower) on the surface. (b) Metal foil without BmimFeCl$_4$ (upper) and with BmimFeCl$_4$ (lower) on the surface after 40 days. (c) Ni foil without BmimFeCl$_4$ (upper) after 40 days and Ni foil treated with BmimFeCl$_4$ for 40 days after cleaning BmimFeCl$_4$ from the surface (lower).



**Figure 10.** CV test of a C-Fe graphite full cell: (a) at the voltage ranging from −1 to 1 V and (b) at the voltage ranging from −1.5 to 1.5 V. Reference electrode: Ag.

of the IL are shown in Figure 1. It illustrates that the density of the IL decreased with an increase in the temperature between 20 and 80 °C. In addition, it was shown that BmimFeCl$_4$ has a high density. This property is good when ILs are utilized as an electrolyte in a battery. It means that for the same mass, BmimFeCl$_4$ will take up less volume.

**Measurement of Viscosity and Rheological Properties.** The viscosity and rheological properties of BmimFeCl$_4$ were measured at a temperature of 20 °C. The results are shown in Figure 2. BmimFeCl$_4$ has lower viscosity values compared with conventional ILs. Low viscosity is advantageous since the ions can drift easily between the electrodes. In addition, as shown in Figure 2, the viscosity of the IL BmimFeCl$_4$ decreases with an increasing temperature, ranging

from 10 to 50 °C, which is in agreement with the viscosity vs temperature trend of conventional ILs.

**DSC Curve Measurement.** The melting point of BmimFeCl$_4$ was measured by DSC. The DSC curve of BmimFeCl$_4$ is shown in Figure 3. It illustrates that BmimFeCl$_4$ has a very low melting point, namely, ca. −85 °C. This means that the BmimFeCl$_4$ electrolyte can be utilized in very low temperature areas and applications, for example, in the harsh cold Arctic/Antarctic areas. In addition, a low melting point is also good to utilize the battery for future space technology development.

**TGA Curve Measurement.** The thermal stability of the BmimFeCl$_4$ electrolyte was measured by TGA. The TGA curves are shown in Figure 4. It is shown that the IL BmimFeCl$_4$ has high thermal stability, and its decomposition temperature is ca. 459 °C. This means that BmimFeCl$_4$ has excellent thermal stability for electrolyte applications, which leads to the BmimFeCl4-based battery having extremely high safety properties. This BmimFeCl$_4$ electrolyte is not oxygen- or

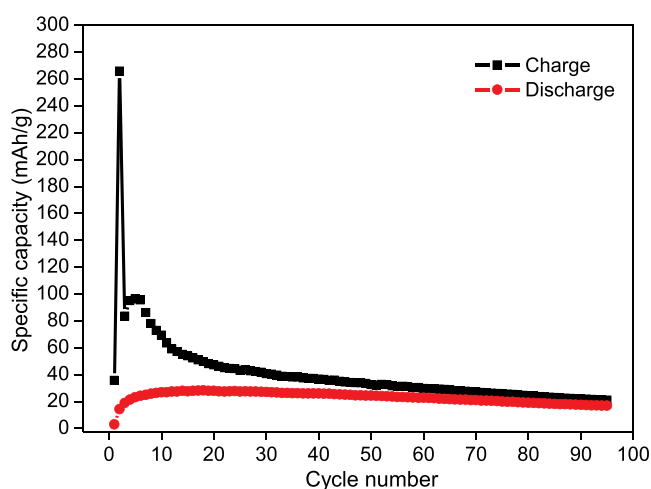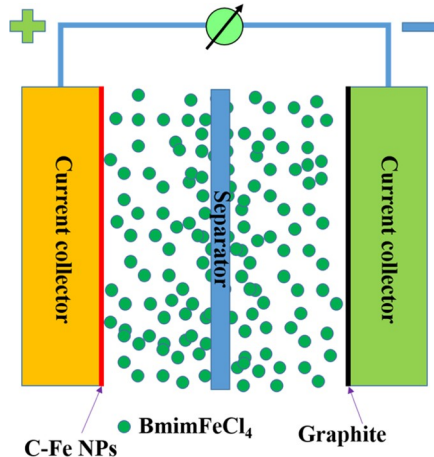## Scheme 1. Structure of a Rechargeable Fe-Ion Battery



**Figure 11.** Charge−discharge test of a Fe ion cell.

water-sensitive and not flammable. In addition, the cost of this BmimFeCl$_4$ is low.

**Raman Analysis.** The chemical structure of magnetic ILs of BmimFeCl$_4$ and OmimFeCl$_4$ is characterized by Raman analysis. The results are shown in Figure 5. The spectra of BmimFeCl$_4$ and OmimFeCl$_4$ showed a strong band at 330 cm$^{-1}$, which was assigned to the totally symmetric Fe−Cl stretch variation of FeCl$_4^-$. It illustrates that there is a FeCl$_4^-$ function group in the two ILs. This means that BmimFeCl$_4$ and OmimFeCl$_4$ are synthesized and obtained.

**Ionic Conductivity Measurement.** The ionic conductivity of magnetic IL electrolytes was measured using an ionic conductivity meter. The results are shown in Figure 6, which illustrates that BmimFeCl$_4$ has good ionic conductivity. In addition, as shown in Figure 6, the ionic conductivity of BmimFeCl$_4$ increased with an increase in the temperature.

**Electrochemical Window Measurement.** The electrochemical window of BmimFeCl$_4$ was measured using a VMP. The results are shown in Figure 7. It illustrates that the electrochemical window of BmimFeCl$_4$ is from −2.1 to 1.9 V vs Ag/Ag$^+$. Consequently, the electrochemical window of BmimFeCl$_4$ was wide enough to be utilized as an electrolyte for the fabrication of the Fe-ion battery.

**Current Collector Selection.** A CV test of a Ni symmetric cell with pure BmimCl$_4$ as the electrolyte was performed. The CV curve is shown in Figure 8. It is shown that the IL BmimFeCl$_4$ is reversible in the Ni symmetric cell. Therefore, this means that the Ni foil can be an option to be utilized as a current collector for the preparation of Fe-ion battery electrodes.

**Corrosion Test.** The corrosion effect of BmimFeCl$_4$ on Cu, Al, and Ni foils was investigated. The corrosion experiment was performed over a period of 40 days in air and at room temperature. The test results are shown in Figure 9a−c. It is shown that BmimFeCl$_4$ can have a chemical reaction with Cu or Al. However, for a Ni foil, only a minor chemical reaction can be seen. Therefore, Ni is utilized in the fabrication of the Fe-ion battery.
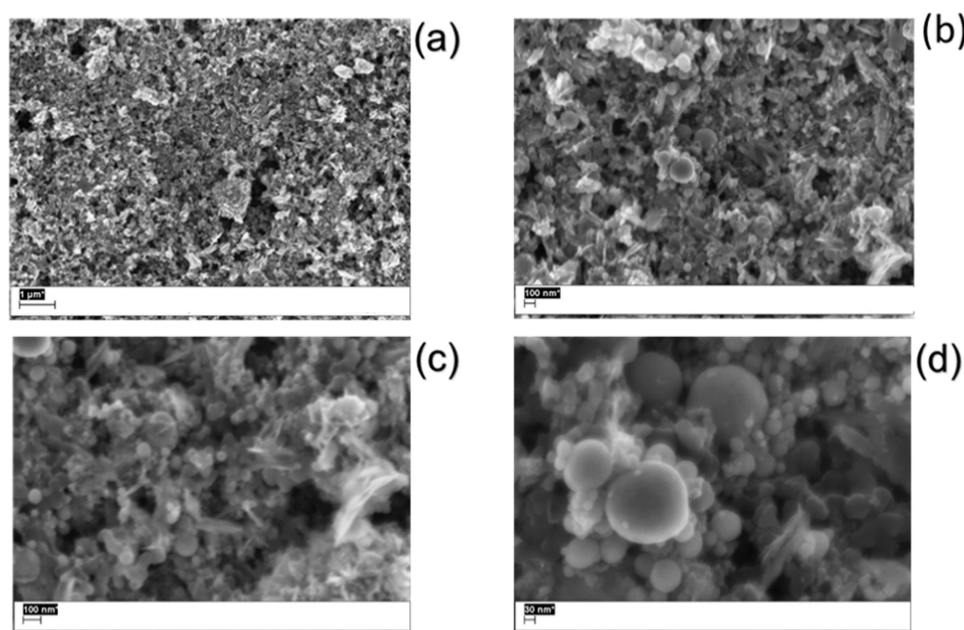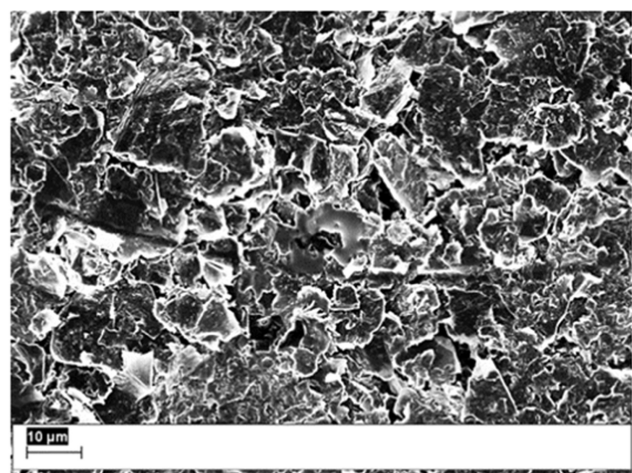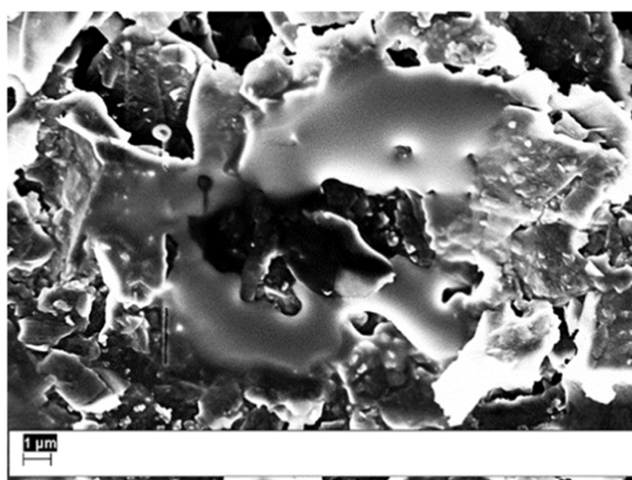


**Figure 12.** SEM of a fresh C-Fe electrode: (a) ×10 000; (b) ×30 000; (c) ×50 000; and (d) ×10 0000.
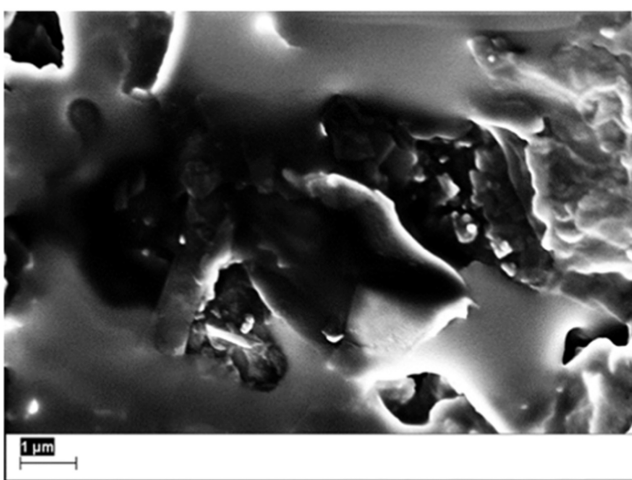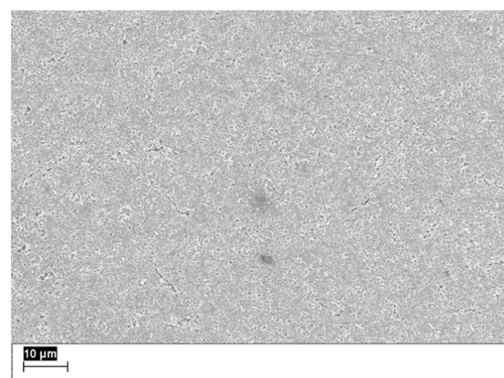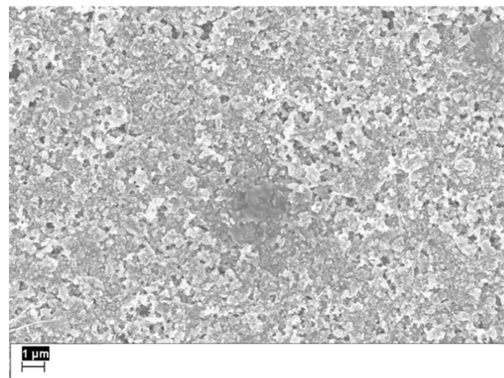
(a)



(b)



(c)

**Figure 13.** SEM of the used C-Fe electrode from the cell after charge and discharge cycles: (a) ×1000; (b) ×5000; and (c) ×10 000.



(a)



(b)



(c)



(d)

**Figure 14.** SEM of a used C-Fe anode from a cell with a graphite cathode after charge and discharge cycles. (a) ×1000; (b) ×5000; (c) ×10 000; and (d) ×20 000.
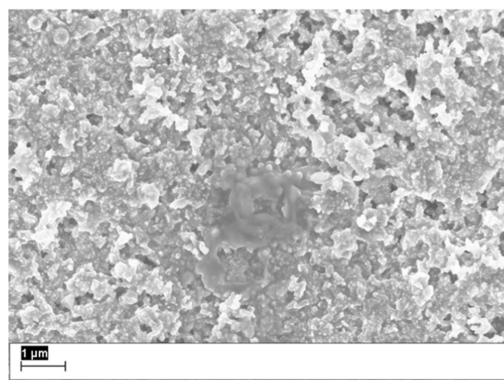
**CV Test of Full Cells.** C-Fe graphite full cells were prepared for the CV test. The electrolyte in the full cells was BmimFeCl$_4$. CV test results of the C-Fe graphite full cell are shown in Figure 10. It is shown that the C-Fe graphite full cell is completely reversible at −1.5 to 1.5 V.
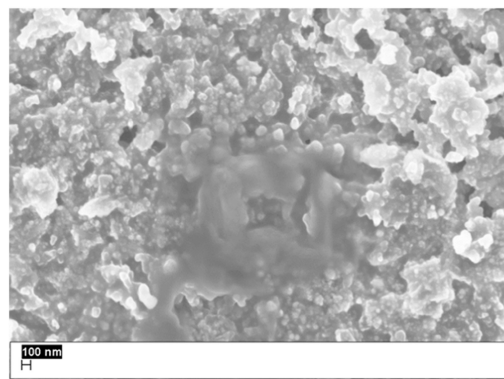
**Fe-Ion Battery.** The structure of a Fe-ion battery is shown in Scheme 1. The electrolyte utilized in the battery is magnetic

IL BmimFeCl$_4$. Fe element-containing materials are utilized as the cathode in this work. Graphite is utilized as the anode in the Fe-ion battery. The proposed working mechanism of the Fe-ion battery is due to the movement of Fe$^{3+}$ between the cathode and anode during the charge and discharge processes. This mechanism is similar to Li$^+$ movement in Li-ion batteries during the charge and discharge processes.[17,18]

**Charge and Discharge of Full Cell.** A charge and discharge test of a full Fe-ion battery was performed. The results are shown in Figure 11. The discharge and charge capacity of this cell was around 20−100 mAh/g during the first 100 cycles.

**SEM.** SEM pictures of the anode are shown in Figures 2−4. As shown in Figure 12, the C-Fe NPs are found on the surface of the electrode. However, as shown in Figure 13, after charge−discharge cycles, the C-Fe NPs are changed and instead form larger-sized structures. This means that the Fe in the C-Fe NPs is active in the charge and discharge process, which also means that we can utilize the C-Fe NPs electrode as a cathode. As shown in Figure 14, the surface of the C-Fe NP anode used as a counter electrode in the Swage-type cell, almost does not change. This means that we should use the C-Fe NP electrode as a cathode and not as an anode.

## CONCLUSIONS

ILs can be utilized as electrolytes in batteries and super-capacitors. Therefore, in this work, the physical and electro-chemical properties of IL electrolytes were investigated using a density meter, rheometer, conductivity meter, DSC, TGA, SEM, and electrochemical instrument. Based on the exper-imental results, it was found that BmimFeCl$_4$ has good properties to be utilized as electrolytes. Therefore, BmimFeCl$_4$ was selected for the Fe-ion rechargeable battery.

The Fe-ion battery can be potentially utilized in stationary energy storage devices, buildings, railways, electrical cars, electric ships, mobile devices, space technology, and other large-scale energy storage systems. Fe is the cheapest metal among all of the metallic materials. There is plenty of mineable Fe on the earth. The cost of the Fe-ion battery was potentially much lower compared with Li-ion batteries. The Fe-ion battery is also an extremely safe battery. Electrodes inside the Fe-ion battery are not oxygen- or water-sensitive. The Fe-ion battery is highly stable, and there is no explosion risk. Importantly, for the Fe-ion battery obtained in our laboratory, a pure IL is utilized as the electrolyte to replace the organic solvents in traditional batteries. ILs have many favorable physical and chemical properties, such as nonflammability, high decom-position temperature, low vapor pressure, high ionic conductivity, and a good electrochemical window.

The cathode of Fe-ion battery consists of Fe-containing materials, including a pure Fe foil, C-Fe NPs, and Fe powder. Various types of Fe-ion full cells were obtained in the laboratory. It was found that the Fe-ion battery with the C-Fe NP cathode and BmimFeCl$_4$ electrolyte showed good performance. The electrochemical properties of Fe-ion full cell were investigated, including CV curves and charge−discharge capacity. To understand the charge−discharge mechanism of the Fe-ion battery, SEM was utilized to investigate the electrode surface before and after utilization of the cells. The Fe-ion battery is also a magnetic battery. There may be other potential applications due to the magnetic properties of the Fe-ion batteries and the nonvolatile electrolyte inside of the Fe-ion battery.

## AUTHOR INFORMATION

### Corresponding Author

**Yansong Zhao** − *Department of Safety, Chemistry and Biomedical Laboratory Sciences, Faculty of Engineering and Science, Western Norway University of Applied Sciences (HVL), 5020 Bergen, Norway;* ⊙ orcid.org/0000-0003-2553-4765; Email: yansong.zhao2004@gmail.com, yansong.zhao@hvl.no

### Authors

**Yingpeng Zhen** − *Department of Civil and Environmental Engineering, Norwegian University of Science and Technology (NTNU), NO-7491 Trondheim, Norway*

**Tobias Boström** − *Renewable Energy Group, Department of Physics and Technology, UiT The Arctic University of Norway, NO-9037 Tromsø, Norway*

Complete contact information is available at:
https://pubs.acs.org/10.1021/acsomega.1c06170

### Notes

The authors declare no competing financial interest.

## REFERENCES

(1) Pan, H.; Hu, Y.; Chen, L. Room-temperature stationary sodium-ion batteries for large-scale electric energy storage. *Energy Environ. Sci.* **2013**, *6*, 2338−2360.

(2) Zu, C.-X.; Li, H. Thermodynamic analysis on energy densities of batteries. *Energy Environ. Sci.* **2011**, *4*, 2614−2624.

(3) Hartmann, P.; Bender, C.; Vračar, M.; Dürr, A.; Garsuch, A.; Janek, J.; Adelhelm, P. A rechargeable room-temperature sodium superoxide (NaO$_2$) battery. *Nat. Mater.* **2013**, *12*, 228−232.

(4) Aurbach, D.; Lu, Z.; Schechter, A.; Gofer, Y.; Gizbar, H.; Turgeman, R.; Cohen, Y.; Moshkovich, M.; Levi, E. Prototype systems for rechargeable magnesium batteries. *Nature* **2000**, *407*, 724−727.

(5) https://en.wikipedia.org/wiki/Abundance_of_elements_in_Earth%27s_crust (accessed February, 2022).

(6) https://en.wikipedia.org/wiki/Oddo%E2%80%93Harkins_rule (accessed February, 2022).

(7) Hoogerstraete, V.; Binnemans, K. Highly efficient separation of rare earths from nickel and cobalt by solvent extraction with the ionic liquid trihexyl(tetradecyl)phosphonium nitrate: a process relevant to the recycling of rare earths from permanent magnets and nickel metal hydride batteries. *Green Chem.* **2014**, *16*, 1594−1606.

(8) Wellens, S.; Thijs, B.; Binnemans, K. An environmentally friendlier approach to hydrometallurgy: highly selective separation of cobalt from nickel by solvent extraction with undiluted phosphonium ionic liquids. *Green Chem.* **2012**, *14*, 1657−1665.

(9) Asadi, M.; Kim, K.; Liu, C.; Addepalli, A.; Abbasi, P.; Yasaei, P.; Phillips, P.; Behranginia, A.; Cerrato, J.; Haasch, R.; Zapol, P.; Kumar, B.; Klie, R.; Abiade, J.; Curtiss, L.; Salehi-Khojin, A. Nanostructured transition metal dichalcogenide electrocatalysts for CO$_2$ reduction in ionic liquid. *Science* **2016**, *353*, 467−470.

(10) Rosen, B.; Salehi-khojin, A.; Thorson, M.; Zhu, W.; Whipple, D.; Kenis, P.; Masel, R. Ionic Liquid−Mediated Selective Conversion of CO$_2$ to CO at Low Overpotentials. *Science* **2011**, *334*, 643−644.

(11) Lei, Z.; Chen, B.; Koo, Y.; MacFarlane, D. Introduction: Ionic Liquids. *Chem. Rev.* **2017**, *117*, 6633−6635.

(12) Kawano, R.; Matsui, R.; Matsuyama, C.; Sato, A.; Susan, M.; Tanabe, N.; Watanabe, M. High performance dye-sensitized solar cells using ionic liquids as their electrolytes. *J. Photochem. Photobiol.* **2004**, *164*, 87−92.

(13) Basile, A.; Bhatt, A.; O'Mullane, A. Stabilizing lithium metal using ionic liquids for long-lived batteries. **2016**, *7*, ncomms11794. DOI: 10.1038/ncomms11794.

(14) Kim, T. Y.; Lee, H.; Stoller, M.; Dreyer, D.; Bielawski, C.; Ruoff, R.; Suh, K. High-Performance Supercapacitors Based on Poly(ionic liquid)-Modified Graphene Electrodes. *ACS Nano* **2011**, *5*, 436−442.

(15) Zhao, Y.; Boström, T.; Passerini, S.; Moretti, A.; Bresser, D.; Zhen, Y. Rechargeable Iron-ion Battery. WO202007911.

(16) Zhao, Y.; Hansen, J.; Boström, T. Extraction of magnetic nanoparticles using magnetic ionic liquids. *IET Micro Nano Lett.* **2015**, *11*, 244−247.

(17) Li, J.; Li, F.; Zhang, L.; Zhang, H.; Lassi, U.; Ji, X. Recent applications of ionic liquids in quasi-solid-state lithium metal batteries. *Green Chem. Eng.* **2021**, *2*, 253−265.

(18) Song, X.; Wang, C.; Chen, J.; Xin, S.; Yuan, D.; Wang, Y.; Dong, K.; Yang, L.; Wang, G.; Haitao Zhang, H.; Zhang, S. Unraveling the Synergistic Coupling Mechanism of $Li^+$ Transport in an "Ionogel-in-Ceramic" Hybrid Solid Electrolyte for Rechargeable Lithium Metal Battery. *Adv. Funct. Mater.* **2021**, No. 2108706.